Structural basis of malaria RIFIN binding by LILRB1-containing antibodies

Yiwei Chen[#1,2], **Kai Xu**[#3], **Luca Piccoli**[1], **Mathilde Foglierini**[1,4], **Joshua Tan**[1], **Wenjie Jin**[1,2], **Jason Gorman**[3], **Yaroslav Tsybovsky**[5], **Baoshan Zhang**[3], **Boubacar Traore**[6], **Chiara Silacci-Fregni**[1], **Claudia Daubenberger**[7], **Peter D. Crompton**[8], **Roger Geiger**[1], **Federica Sallusto**[1,2], **Peter D. Kwong**[3], **Antonio Lanzavecchia**[1,9,✉]

[1]Institute for Research in Biomedicine, Università della Svizzera italiana, Via Vincenzo Vela 6, 6500 Bellinzona, Switzerland [2]Institute of Microbiology, ETH Zurich, Wolfgang-Pauli-Strasse 10, 8093, Zurich, Switzerland [3]Vaccine Research Center, National Institute of Allergy and Infectious Diseases, National Institutes of Health, Bethesda, Maryland 20892, USA [4]Swiss Institute of Bioinformatics (SIB), Lausanne, Switzerland [5]Electron Microscopy Laboratory, Cancer Research Technology Program, Leidos Biomedical Research Inc., Frederick National Laboratory for Cancer Research, Frederick, Maryland 21701, USA [6]Malaria Research and Training Center, Department of Epidemiology of Parasitic Diseases, International Center of Excellence in Research, University of Sciences, Techniques and Technologies of Bamako, Bamako, Mali [7]Swiss Tropical and Public Health Institute, University of Basel, Basel, Switzerland [8]Laboratory of Immunogenetics, National Institute of Allergy and Infectious Diseases, National Institutes of Health, Rockville, MD, USA

[#] These authors contributed equally to this work.

Abstract

We previously reported that certain *Plasmodium falciparum* RIFINs, variant surface antigens expressed on infected erythrocytes[1], bind to the inhibitory receptor LAIR1 and insertions of DNA encoding LAIR1 into immunoglobulin genes generate RIFIN-specific antibodies[2,3]. To address the general relevance of this finding, we searched for antibodies that incorporate LILRB1, another inhibitory receptor that binds to β2 microglobulin and RIFINs through their apical domains[4,5]. By screening plasma from a Malian cohort, we identified individuals with LILRB1-containing antibodies. B cell clones isolated from three donors showed large DNA insertions in the switch

region encoding non-apical LILRB1 D3D4 or D3 alone in the variable-constant (VH-CH1) elbow. Through mass-spectrometry and binding assays, we identified a large set of RIFINs that bind to LILRB1 D3. The crystal and cryo-EM structures of a RIFIN in complex with either LILRB1 D3D4 or a D3D4-containing antibody Fab revealed a mode of RIFIN-LILRB1 D3 interaction comparable to that of RIFIN-LAIR1 (Xu et al, in press). Remarkably, the Fab showed an unconventional triangular architecture with the inserted LILRB1 domains opening up the VH-CH1 elbow without affecting VH-VL nor CH1-CL pairing. Collectively, these findings identify a new modality of RIFIN binding to LILRB1 through D3 and illustrate, with a naturally selected example, the general principle of creating novel antibodies by inserting receptor domains in the VH-CH1 elbow.

Repetitive interspersed families of polypeptides (RIFINs) are variable antigens expressed on infected erythrocytes (IE) and are encoded by a large number of polymorphic *P. falciparum* genes[6]. RIFINs mediate aggregation and rosette-formation thus contributing to the pathogenesis of severe malaria[1]. We previously reported that certain RIFINs bind to the collagen-specific inhibitory receptor LAIR1, suggesting a role in immune evasion[2,3]. A subsequent study[7] confirmed our observation and suggested that RIFINs could bind to multiple inhibitory receptors on myeloid and lymphoid cells, in particular to LILRB1, an inhibitory receptor that binds to β2m through its apical N-terminal domains (D1D2)[4]. The interaction of RIFINs with LILRB1 has been recently supported by the structure of RIFIN (PF3D7_1254800) bound to the D1D2 interface, which mimicked avidity-based interactions with β2m[5].

Natural LILRB1-containing antibodies

Based on the discovery of LAIR1-containing antibodies in malaria-exposed individuals[2,3], we hypothesized that B cell clones with insertions of other inhibitory receptors recognized by the parasite, such as LILRB1, could be selected in the course of malaria infection. We therefore screened 672 plasma samples from a Malian cohort[8] and identified 6 individuals with LILRB1-containing IgG (Fig. 1a). From three positive donors (MDA, MDB, MDC), we isolated B cell clones producing LILRB1-containing monoclonal antibodies that bound to IE (Fig. 1b). As previously found for LAIR1-containing antibodies, in each donor the isolated B cells belonged to a single clonal family as demonstrated by identical inserts and VDJ rearrangements (Extended Data Fig. 1, Extended Data Fig. 2 and Supplementary Table 1). In all cases, templated *LILRB1* insertions were found between VDJ and CH1 and comprised, in MDA and MDB clones, *LILRB1* exons 7 and 8 (encoding D3 and D4, respectively) and, in MDC clones, exon 7 alone (Fig. 1c-e). Interestingly, while the VH regions were somatically mutated, the LILRB1 inserts were not, except for exon 7 in MDC1, which carried a single Y291D mutation (Extended Data Fig. 2d-e). The lack of somatic mutations is consistent with the fact that LILRB1 D3 is not self-reactive, unlike the collagen-binding LAIR1 domain which was always found to have mutated away from self-reactivity when inserted in antibody genes[3].

Sequencing of gDNA from representative B cell clones showed long and complex genomic inserts (Fig. 1c-e and Extended Data Fig. 3). In donor MDA, the antibody was an IgG1 and

the insert was found in the switch μ region and comprised a 1271 bp *LILRB1* genomic fragment spanning exons 6, 7 and 8. In donor MDB, the antibody was an IgG4 and the insert was found in the switch γ1 region and comprised a 1723 bp genomic fragment spanning exons 7, 8 and 9 with flanking intronic sequences plus a short inverted sequence derived from exon 2 at the 5' end. Finally, in donor MDC, the antibody was an IgG3 and the insert was in the switch μ region and comprised a shorter 645 bp fragment spanning exon 7 with flanking intronic sequences plus a small portion of exon 6. Importantly, the conservation of the splice sites flanking exons 7 and 8 allowed, in all cases, the precise splicing observed in the cDNA.

Consistent with the cDNA data, Western blot analysis of the antibodies secreted by the B cell clones revealed the presence of a heavy chain of higher MW that was blotted by anti-LILRB1 polyclonal antibodies (Fig. 1f). Strikingly, this was the only form of heavy chain present in the B cell culture supernatant of the MDA1 and MDC1 B cell clones, suggesting a very high efficiency of LILRB1 exons splicing in these cells. Collectively, these findings provide, after LAIR1[3], a second example of antibodies generated by templated insertions in the switch region that rely on efficient splicing of inserted exons.

LILRB1 binds to a specific set of RIFINs

To identify the targets of LILRB1-containing antibodies, we performed multiple rounds of enrichment of 3D7-IEs using the MDB1 antibody as a bait and isolated by cell sorting MDB1^{+} and MDB1^{-} IEs (Fig. 2a). LC-MS/MS revealed the presence of several RIFINs, of which three (PF3D7_1373400, PF3D7_0937700, PF3D7_1041200) were highly enriched in the MDB1^{+} fraction (Fig. 2b and Extended Data Fig. 4). Staining of HEK cells transfected with RIFIN V2 domains confirmed specific binding of LILRB1-containing antibodies to the 3 RIFINs that were differentially expressed (Fig. 2c). Given the limited levels and diversity of RIFIN expression in cultured parasites, possibly due to lack of selective pressure, we used a homology-based approach to identify additional LILRB1-binding RIFINs. The alignment of the 3 positive RIFINs identified 14 shared hotspots in the V2 region that defined a low-resolution LILRB1 binding signature (Fig. 2d). This signature was used to screen in silico the remaining 221 3D7 RIFINs, which were ranked according to the number of shared hotspots. For each rank, 1 or 2 RIFINs were expressed and tested. Using this approach, we identified four additional 3D7 RIFINs that were recognized by LILRB1-containing antibodies, namely PF3D7_0632400, PF3D7_0324800, PF3D7_1041000 and PF3D7_1300700 (Fig. 2e and Extended Data Fig. 4d-e). Finally, using the new set of 7 LILRB1 positive RIFINs, we defined a higher resolution signature that was applied to predict 141 LILRB1-specific RIFINs of other parasite strains out of the 2732 present in the current databases (Source Data Extended Data Fig. 4). Interestingly, phylogenetic analysis shows that LILRB1-specific RIFINs are distinct from the LAIR1-specific RIFINs as they are found in different branches of the phylogenetic tree (Fig. 2f, Extended Data Fig. 5 and Extended Data Fig. 6).

RIFIN binding maps to LILRB1 D3 domain

To dissect the LILRB1 domains involved in binding to different RIFINs, we tested a panel of RIFIN transfectants with natural and recombinant antibodies and fusion proteins containing different LILRB1 domains (Fig. 3a and Extended Data Fig. 7). Antibodies containing LILRB1 D3/D4 or D3 inserts bound to the 7 identified RIFINs, while deletion of the inserted domains completely abolished binding, indicating a critical role for D3. In contrast, recombinant antibodies containing LILRB1 D1/D2 or D4 inserts did not bind to any RIFIN tested, including PF3D7_1254800 and PF3D7_0223100 that were recently reported to bind to D1D2[5], a finding that may be related to avidity requirements and very low affinity of this interaction. Furthermore, an Ig fusion protein containing all the 4 LILRB1 domains bound to all 7 RIFINs, demonstrating D3-mediated binding to be independent of the molecular context. Finally, binding of D3 containing antibodies was also demonstrated using full length RIFINs displayed on IE (Fig. 3b). Collectively, the above experiments identify a set of seven RIFINs that are targeted by LILRB1 D3-containing antibodies. Interestingly, these RIFINs differ from those that bind to LILRB1 D1D2 domains[5], suggesting distinct binding modalities.

Structure of a LILRB1-Fab bound to RIFIN

To visualize the LILRB1 D3D4 insert in the context of the antibody molecule and the interaction of D3 with RIFINs, we determined a cryo-EM structure of MDB1 Fab in complex with V2 domain of RIFIN PF3D7_1373400 at 3.5 Å resolution (Fig. 4a, Extended Data Fig. 8, and Supplementary Table 2). The structure revealed an unconventional triangular shape Fab architecture due to the elbow insertion of LILRB1 D3D4 domains. The VH/VL, D3D4 and CH1/CL domains compose the three apexes of the triangle and their structures superimpose well with their original structures individually (Extended Data Fig. 9a). In particular, the angle of light chain elbow region swings outward almost 90° degrees, to accommodate the LILRB1 D3D4 insertion in the heavy chain elbow region. In addition, MDB1 Fab formed a homodimer through the interaction between the two light chains, as well as between VH and D3D4 insertion on the other copy of MDB1 Fab. Consistent with the mapping data, the structure indicated that RIFIN V2 interacted only with the LILRB1 D3 domain. Due to inter-domain flexibility of MDB1-RIFIN complex revealed by 3D variability analysis, except the region around MDB1-RIFIN interface, the reconstruction density for RIFIN was less clear. We therefore exploited X-ray crystallographic approach to determine the structure of complex between LILBR1 D3D4 domain and RIFIN PF3D7_1373400 V2 domain to 2.6 Å resolution, which provided a clear view of entire RIFIN molecule and the LILBR1-RIFIN interface (Fig. 4b, c).

The interface of MDB1-RIFIN is formed by the RIFIN V2 apex region and one side of LILRB1 D3 immunoglobulin (Ig) like domain β-sandwich. RIFIN V2 apex region involves α5 helix and its two adjacent loops. The contacting side of LILRB1 D3 domain involves the strands C, C' and F, together with the neighboring loop regions. The interface is composed of mostly hydrophobic interaction, which involves the side chain contact between RIFIN residues L243, P244, V246, P253, P255, A259, L272, L278 and LILRB1 residues Y258, L268, Y298, L303, W307. However, hydrophilic interactions also play important roles,

including the salt-bridges of $D268_{RIFIN}$-$R254_{LILRB1}$ and $K280_{RIFIN}$-$D264_{LILRB1}$, the hydrogen bond formed between $F248_{RIFIN}$ main chain carbonyl and $R168_{MDB1}$ side chain guanidium group, and the intermolecular β-strand hydrogen bonding formed between α5-α6 region of RIFIN and C' strand of LILRB1 D3 domain. Four glycine and six proline residues in RIFIN α4-α5 loop region, including P244, P247, G250, G251, P252, P253, P255, G256, G258 and P262, increase the flexibility of α4-α5 loop and enable a better fit to the hydrophobic groove on LILRB1 D3 domain.

The structure of the RIFIN PF3D7_1373400-LILRB1 D3 complex resembled that of RIFIN PF3D7_1040300-LAIR1 complex described by Xu et al (in press) (Extended Data Fig. 9b). In both cases, RIFINs target to C-C' and surrounding regions on Ig like domain. Remarkably, these structures are completely different from that reported for RIFIN PF3D7_1254800-LILRB1 D1D2 complex where the interaction is limited to D1D2 interface[5]. Nevertheless, the two structures of LILRB1-RIFIN complexes revealed that the V2 apex is the common binding site utilized by RIFINs to bind different domains of the same receptor (Extended Data Fig. 9c).

The LILRB1-containing antibodies described in this study provide a new example of natural selection and clonal expansion of rare B cells with functional inserts in antibody genes and illustrate the general principle of receptor-based antibodies. Although functional in-frame insertions can be found between V and DJ segments, as in the case of LAIR1[2,9], the switch region emerges as a particularly permissive site for functional insertions, due to the efficiency of exon splicing and to the flexibility of the Ig elbow that can accommodate up to two Ig domains. The structure of the LILRB1 D3D4-containing Fab reveals a new mechanism, with the light chain elbow acting as a hinge that swings outward to accommodate insertions of different size in the VH-CH1 elbow. This property can be exploited to create bispecific antibodies by insertion of VHH, scFv or pathogen receptor domains.

Together with a recent report[5], our results provide new insights into the role of RIFINs in immune evasion. The finding that phylogenetically distinct RIFINs target LILRB1 D1D2 and LILRB1 D3 provides a striking example of convergent evolution, as well as redundancy. The structures of RIFINs bound to LAIR1 and LILRB1 D3 illustrate a common interaction modality with the lateral site of the inhibitory receptor Ig domains and are strikingly different from the RIFIN-LILRB1 D1D2 structure recently reported that would be consistent with RIFIN mimicking β2m[5]. The fact that we did not find antibodies with insertions of LILRB1 D1D2 may be related to the low affinity of D1D2-RIFIN interaction and to the requirement for somatic mutations that would remove self-reactivity with β2m. Overall, the striking polygenicity and polymorphism of the RIFIN family is consistent with a strong selective pressure for evading the antibody response while developing different ways to bind to inhibitory receptors[10], a mechanism that can be effectively countered by receptor-based antibodies (Extended Data Fig. 10).

Methods

Serum plasma samples and cells

No statistical methods were used to predetermine the sample size. The experiments were not randomized, and the investigators were not blinded to allocation during experiments and outcome assessment. The majority of the Malian sera were obtained from a cohort in Kalifabougou, Mali[11], which has high malaria transmission levels from June to December. This cohort consists of both children and adults, ranging from 3 months to 25 years. The samples that were tested were obtained just after the malaria transmission season. Smaller numbers of sera were also obtained from adults in the Fulani and Dogon ethnic groups in Mantéourou, Mali, who were initially enrolled in a study testing the immunological basis of enhanced protection of members of the Fulani ethnic group to malaria[8]. Healthy individuals' sera samples were obtained from adults (various ages and genders) in the Canton Ticino, Switzerland.

Ethics approval

The Mali study was approved by The Ethics Committee of the Faculty of Medicine, Pharmacy and Dentistry at the University of Sciences, Technique and Technology of Bamako, and the Institutional Review Board of the National Institute of Allergy and Infectious Diseases, National Institutes of Health. Written informed consent was obtained from participants or parents or guardians of participating children before inclusion in the Mali study. Sera from healthy individuals are collected based on standard regulation. Each donor gave written informed consent for using these blood samples, following approval by the Cantonal Ethical Committee of Canton Ticino, Switzerland.

Parasite cultures

The *P. falciparum* laboratory line 3D7 clone or other parasites (9215, 9775) used in this study were cryopreserved at the ring stage and was thawed and cultured to 3% parasitemia in blood group O erythrocytes using the following culture medium (RPMI 1640 medium with 10% heat-inactivated serum from healthy donors and supplemented with 25 μg/ml gentamicin, 0.2% glucose, 2 mM L-glutamine, 37.5 mM HEPES and 0.05 mg/ml hypoxanthine). Parasite cultures were routinely tested for Mycoplasma contamination. To select for MDB1-positive infected erythrocytes (IEs), 3D7 IE cultures that have reached to late trophozoite stage were collected into a small volume (1.5 ml) and were incubated with MDB1 (50 ~100 μg/ml) for 30min at room temperature, washed and coated with Protein G magnetic beads (Life Technologies) for 30 min at room temperature. Protein G binding parasites were collected via magnetic sorting and enriched fractions were returned to the *in vitro* culture. After 24 hours, the magnetic beads were removed from the parasite culture and discarded[2]. The enrichments were established for several rounds until a clear positive population of MDB-positive 3D7 parasites was observed using the FACS analysis. These enriched population were sustained in *in vitro* culture and used in following LC-MS/MS experiments.

B cell immortalization and isolation of monoclonal antibodies

IgG memory B cells were isolated from donor's frozen PBMCs (peripheral blood mononuclear cells) by first staining with anti-CD19-PECy7 antibodies (BD, 341113) and mouse anti-PE microbeads (Miltenyi Biotec, 130-048-081) and subsequently with a magnetic cell sorting. Enriched CD19^{+} B cells were further stained with Alexa Fluor 647-conjugated goat anti-human IgG (Jackson ImmunoResearch, 109-606-170) for FACS sorting. Sorted B cells were immortalized with Epstein-Barr virus (EBV) and plated in single cell cultures in the presence of CpG-DNA (2.5 μg/ml) and irradiated PBMC-feeder cells. After two weeks, the supernatants of cell culture were tested for the presence of the LILRB1-containing antibody using beads-based immunoassay as described previously[3] and below. To confirm the presence of LILRB1-containing antibody, supernatants of the cell culture were then tested for the capability of binding to parasites. Briefly, fresh or cryopreserved late trophozoite parasites were stained with 10X SYBR Green I for 30 min at room temperature on a rotation rack. The parasites were washed and incubated with the B cell supernatants for 1 hour at 4°C. The antibody binding ability was assessed by FACS staining with 2.5 μg/ml Alexa Fluor 647-conjugated goat anti-human IgG. Similarly, recombinant LILRB1-containing antibodies, antibody constructs (with or without LILRB1 domains), or control antibodies were applied to the parasites for the FACS staining. Parasites binding curves in Fig. 1b was generated using series dilution of recombinant LILRB1-containing antibodies staining with 9605 parasite isolates, and the mean fluorescence intensity (MFI) was collected in Flow-jo and analyzed in GraphPad Prism 8. Specifically, curves of the recombinant LILRB1-containing antibodies binding to parasites were generated by fitting data to a non-linear regression model using GraphPad Prism 8. FACS staining of 9775 IEs in Fig. 3b with natural or engineered antibody were using the same methods.

Screening of LILRB1-containing antibodies with bead-based immunoassay

Serum and plasma were tested for the presence of LILRB1-containing antibodies using a two-determinant bead-based immunoassay as described previously[3]. Briefly, anti-goat IgG microbeads (Spherotech) were coated with goat anti-human LILIRB1 (R&D Systems, AF2017) and 40 × SYBR Green I (ThermoFisher Scientific) or with goat anti-human EGF (R&D Systems, AF-259-NA) without SYBR Green I for 20 min at room temperature. The beads were washed, mixed, and incubated with the serum for 1 hour at room temperature. Beads coated with anti-LILRB1 were differentiated from control beads coated with anti-EGF based on SYBR green staining. Serum antibody binding was detected using 2.5 μg/ml Alexa Fluor 647-conjugated donkey anti-human IgG (Jackson ImmunoResearch, 709-606-098). FACS Diva (version 6.2) was used to acquire samples, and Flow-Jo (version 10.1) was used for flow cytometry analysis. MFI% was calculated by subtracting the MFI of the anti-EGF control beads from that of the anti-LILRB1 beads in the IgG channel then divided by the MFI of anti-LILRB1 beads. The cutoff was set at no differences (MFI% = 0). The error bars were calculated using GraphPad Prism 8, indicating the standard deviation within the group Malian or European.

Sequence analysis of monoclonal antibodies

cDNA of LILRB1-containing antibodies was synthesized from selected B cells, and their heavy chain and light chain sequences were amplified by PCR and sequenced using a specific primer mix as previously described[12]. The usage of variable region genes and somatic mutations accounts were analyzed in IMGT. Genomic DNA was extracted from selected B cell clones using conventional molecular cloning method and was amplified using the REPLI-g Single Cell Kit (QIAGEN) before performing PCR. The insertions of LILRB1 were determined using LILRB1-specific primers and VH specific primers based on cDNA sequences or constant region-specific primers. All the primers used were listed in Supplementary Table 3. After PCR amplification with LongAmp Taq Polymerase (New England Biolabs), the ~6000 bp (VH-CH1) or ~3000 bp (VH-LILRB1, LILRB1-CH1) amplicons were cloned into a TOPO XL vector (TOPO XL PCR cloning kit, ThermoFisher) and sequenced by plasmid-NGS-sequencing (Microsynth, Switzerland).

Western blots

The western blot was performed using standards protocols as previously described[3]. Briefly, B cell supernatants or recombinant antibody constructs were diluted in H_2O, 4x sample loading buffer and 10x sample reducing agent (Life Technologies) were loaded onto precast gels with a 4-12% acrylamide gradient (Invitrogen). The proteins were transferred to PVDF membranes followed by blocking with 5% milk in TBS buffer. The membrane was incubated with primary and secondary antibodies diluted in 2% milk TBS buffer for 1h at room temperature. After washing with the TBS-tween buffer, the membranes were developed using a chemiluminescent substrate (Thermo Scientific). The primary antibodies for detecting IgG or LILRB1 were goat anti-human IgG (SouthernBiotech, 2040-05) used at 2 μg/ml or goat anti-human LILRB1 used at 5 μg/ml (R&D, AF2017). The secondary antibody for both western analyses was rabbit anti-goat HRP used at 0.2 μg/ml (Invitrogen, Catalog 65-6120).

Expression and purification of recombinant antibodies and fusion proteins

The heavy chain and light chain of antibodies (including all the LILBR1-containing antibodies, BKC3, MGD21, and MGDUCA, etc.) were cloned into human IgG1, Igκ or Igλ expression vectors (kindly provided by M. Nussenzweig) and were transfected into the Expi293F cells (ThermoFisher Scientific) using polyethyleneimine (PEI) or Lipofectamine 3000 Reagent (ThermoFisher Scientific). Routine tests for Mycoplasma contamination were performed. The antibodies were affinity purified by protein A chromatography or protein G chromatography using AKTA (Cytiva). Variants of MDB and GCE536 antibody were constructed by inserting or deleting of LILRB1 domains based on the Ensemble genomic database's sequence information. The LILRB1-Fc fusion protein was purchased from R&D Systems (Catalog 2017-T2-050) or produced in the lab. Vectors expressing the LILRB1 domain-containing Fc fusion constructs were gene synthesized by Genscript and expressed in Expi293F cells as described above.

Identification of target antigens by LC-MS/MS

MDB1[+] 3D7 IEs cultures that have reached to late trophozoite stage at >5% parasitemia were enriched using MACS magnetic beads to avoid early-stage parasites. Enriched IEs were stained with 10x SYBR Green I for 30 min at room temperature on a rotation rack. Followed by four times of washing, parasites were stained with 25 μg/ml LILRB1-containing antibody MDB1 at room temperature for 20 min and with 2.5 μg/ml Alexa Fluor 647-conjugated goat anti-human IgG as secondary antibody at the same condition. Subsequently, FACS sorting of MDB1 positive and negative compartments were performed. Positive and negative binding IEs were harvested at 10,000 g for 5 min, then the pellets were treated with hypotonic lysis buffer (5 mM KH_2PO_4, pH 7.4) for the RBC membrane extraction based on the previous protocol (Methods in Malaria Research). The collected RBC membranes were sonicated with Bioruptor® Plus Sonication System (Catalog B01020001) using the following program: 15 cycle, 30s on, 30s off, high. After the sonication, solubilized proteins were treated with a series of chemicals (10 mM DTT, 50 mM IAA, LysC, trypsin, etc.) based on standard mass spectrometry sample preparation procedure[13]. After trypsin digestion, peptides were analyzed on a Q-Exactive instrument at the Institute for Research in Biomedicine. Raw files were analyzed using the MaxQuant software[14], and LC-MS/MS spectra were searched against *P. falciparum* 3D7 UniProt FASTA databases (UP000005640 and UP000001450). Peptide identifications were matched across several replicates. Subsequent data analysis was performed in the R statistical computing environment. The missing values were imputed by a normal distribution with a s.d. of 30% in comparison to the deviation of the measured values and a down-shift of the mean by 1.8 s.d. to simulate the distribution of low abundant proteins. Statistical significance was evaluated by Welch tests. Data were visualized in R studio.

Antigen validation assay

To validate whether certain RIFINs are the antigen recognized by LILRB1-containing antibodies, gene encoding full length or V2 region of RIFIN candidates were produced by gene synthesis (Genescript) and cloned into pDisplay vector (Invitrogen). The vector contains a hemagglutinin (HA) tag, which will be fused to the C-terminal of the RIFIN antigens as previously described[1,2]. RIFIN-containing pDisplay vectors were transiently transfected into HEK293F cells, respectively (ThermoFisher Scientific), using PEI. Cell lines were routinely tested for Mycoplasma contamination. Briefly, one day before transfection, HEK293F cells were seeded at 0.7×10^6 cells/ml in 10 ml Expi293™ Expression Medium (ThermoFisher Scientific). On the day of transfection, 6 μg of construct DNA was diluted in the OPTI-PRO SEM Medium (Invitrogen) and mixed with 60 μg of PEI for 20 min at room temperature. The DNA-PEI complexes were added to the cells, which were cultured in a CO_2 shaker incubator at 37°C, 250 r.p.m. Seventy-two hours post-transfection, cells expressing RIFINs were collected and stained with LILRB1-containing antibodies or control antibodies and tested by flow cytometry. Briefly, 5 μg/ml of LILRB1-containing antibodies were added to the RIFIN-transfected cells for 30 min at 4°C. They were then followed by washing steps before staining with a secondary of 2.5 μg/ml of Alexa Fluor 647-conjugated goat anti-human IgG antibody (Jackson ImmunoResearch, Catalog 109-606-170). The cells were washed for the third time, then stained with 5 μg/ml of rabbit anti-HA tag (Sigma, Catalog H6908) for the same condition followed by washing before

adding the Alexa Fluor 488-conjugated goat anti-rabbit IgG (Life Technologies, Catalog A11034) for the detection of RIFIN.

Sequence Homology analysis

The occurrence of different amino acid identities at the RIFIN-V2 region was analyzed by aligning all RIFIN protein sequences present in the National Center for Biotechnology Information (NCBI) Entrez Protein database[15] as of December 18, 2019, or PlasmoDB database (2008). After alignment of the RIFIN protein sequences using Clustal Ω[16], the V2 region was defined as shown in Extended Data Fig. 4c. We extracted the V2 region of each sequence and aligned them again using Clustal Ω. Hotspots were identified as the shared amino acids between the three LILRB1 binding RIFINs identified in the LC-MS/MS experiment (PF3D7_1373400, PF3D7_0937700 and PF3D7_1041200). The remaining RIFIN protein sequences were analyzed and ranked according to their number of shared hotspots for each position (A191, V196, I197, F204, N222, Y223, A226, I229, F237, P262, I263, C264, I287, V291). Specifically, the numbering of hotspots is relative to PF3D7_1373400 complete protein. In the phylogenetic analyses (Fig. 3f), probabilities of amino acid substitutions are converted to scores of the PAM250 score matrix through conversion to logarithmic values, and all these scores are summed to obtain global similarity scores between any two sequences. The overall average distance tree in Extended Data Fig. 5 assumes a constant rate of evolution across lineages. The average distance trees here were generated using alignments of homologous sequences to infer closest relatives in the context of the gene of interests, and the tree was calculated in MEGA[17]. The alignment of LILRB1 binding RIFINs and LAIR1 binding RIFINs was performed by Clustal Ω and visualized in Jalview. The Percentage Identity in Extended Data Fig. 6 was comparing the similarity of the actual sequences of homologs.

Protein preparation for structural determination

LILRB1 D3D4, antibody MDB1 and RIFIN genes were synthesized and subcloned (GenScript, NJ) into pVRC8400 vectors, with HRV3C cleavable His or Fc tag. DNAs of RIFIN with either LILRB1 or MDB1 were co-transfected into Expi293 Gnti- cells (Thermo Fisher) using Turbo293 transfection reagent (Speed BioSystems). Six days post transfection, culture supernatants were harvested, and affinity purified with cOmplete™ His-Tag Purification Resin (Roche) or protein A resin (GE) by following manufacture's protocols.

Cryo-EM data collection and processing

MDB1-RIFIN complex were treated with HRV3C to remove affinity tags and further purified by SEC with Superdex 200 chromatography column (GE) in the HEPES buffer (5 mM HEPES pH7.5 and 150 mM NaCl), then concentrated to final concentration of 0.5 mg/ml. Sample (2 μl) was applied to a glow-discharged carbon-coated copper grid (CF 1.2/1.3) and vitrified using a Vitrobot Mark IV with a wait time of 30 s and a blot time of 3 s before the grid was plunged into liquid ethane. Data were acquired using the Leginon system[18] installed on Titan Krios electron microscopes operating at 300kV and equipped with K3-BioQuantum direct detection device. The dose was fractionated over 40 raw frames and collected over a 2 s exposure time. Motion correction, CTF estimation, particle picking,

2D classifications, ab initio model generation, heterogeneous refinements, 3D variability analysis and homogeneous 3D refinements were carried out in cryoSPARC[19].

Cryo-EM model fitting

For initial fits to the cryo-EM reconstructed maps, we used the coordinates of LILRB1 D3D4 from PDB ID 4LLA, antibody Fab domains from PDB ID 6P3B and RIFIN PF3D7_1040300 from a companion paper (Xu et al, in press). These initial models were docked into the cryo-EM maps using Chimera[20]. The coordinates were then fit to the electron density more precisely through an iterative process of manual fitting using Coot[21] and real space refinement within Phenix[22], Molprobity[23] and EMRinger[24] were used to check geometry and evaluate structures at each iteration step. Figures were generated in UCSF ChimeraX and PyMOL (https://pymol.org). Map-fitting cross correlations were calculated using Fit-in-Map feature in UCSF Chimera. Overall and local resolution of cryo-EM maps was determined using cryoSPARC.

X-ray crystallographic, data collection and structural determination

To facilitate crystallization, proteins and complexes were treated with HRV3C to remove affinity tags and further purified by SEC with Superdex 200 chromatography column (GE) in the HEPES buffer (5 mM HEPES pH7.5 and 150 mM NaCl). Crystallization conditions were screened using Hampton Research, Wizard, and QIAGEN crystal screening kits. Crystal plates were set up using a Mosquito crystallization robot. Crystals initially observed from the wells were manually reproduced. Optimal crystal grew in 0.1 M Tris 8.3, 11% PEG3350, 1.1 mM AmSO$_4$, 0.2 mM Li$_2$SO$_4$ and was cryoprotected in 25% glycerol and flash-frozen in liquid nitrogen. Data were collected at a wavelength of 1.00 Å at the SER-CAT beamline ID-22 (Advanced Photon Source, Argonne National Laboratory). Diffraction data were processed with the HKL2000 suite. Structural solution was obtained by molecular replacement with Phaser in Phenix using the cryo-EM derived model as search template. Model building was carried out with Coot. Refinement was carried out with Phenix. Data collection and refinement statistics are shown in Supplementary Table 2. The atomic model is available with PDB ID 7KFK.

Statistical information

The number *n* described in the figure legends refers to the number of independent experiments performed with biological replicates. The analysis of LC-MS/MS was performed in *n* = 4 experiments and the statistical significance was evaluated by Welch tests. The error bars were defined in the figure legends if any.

Extended Data
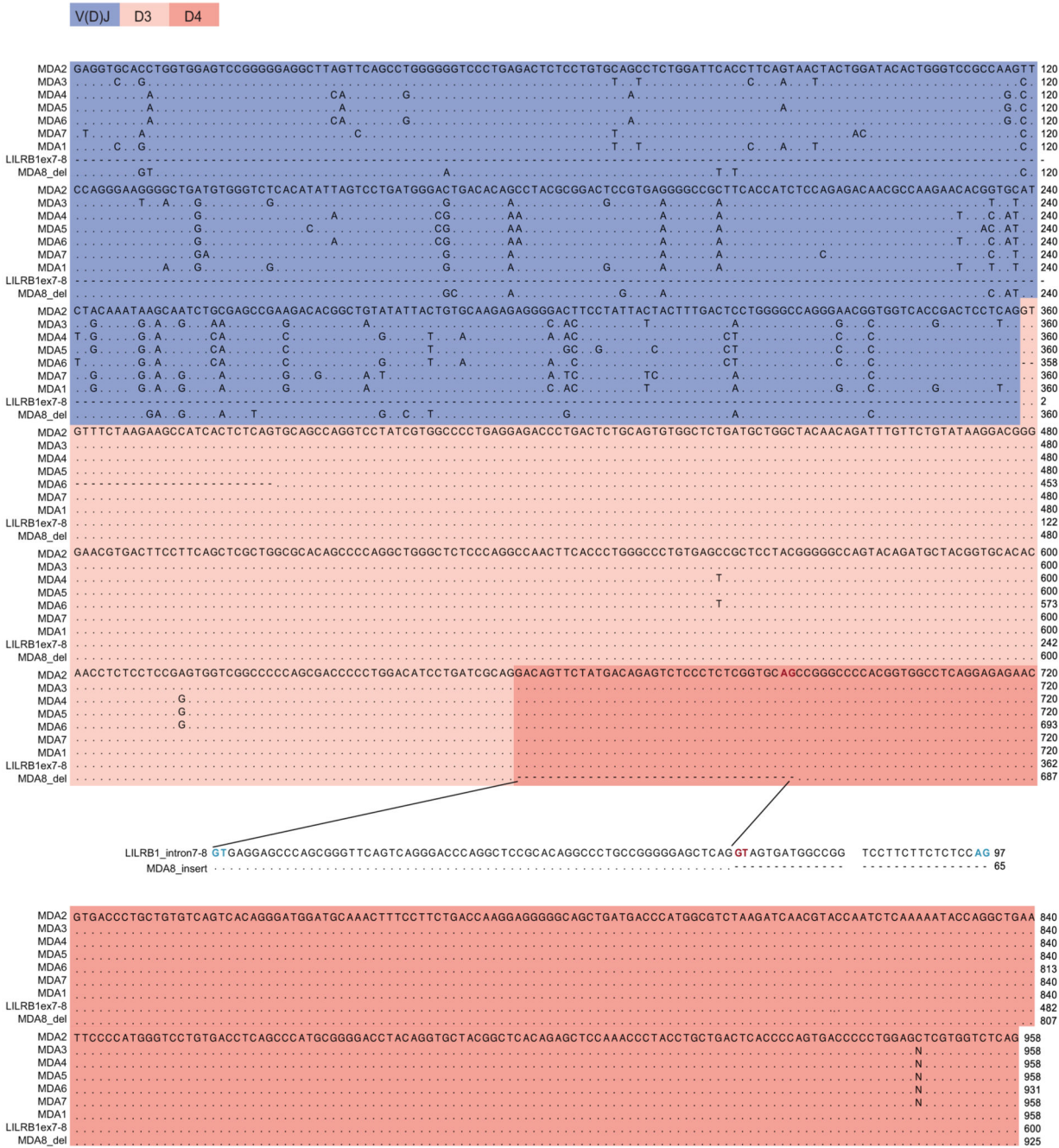
Extended Data Fig. 1. Alignment of cDNA sequences of LILRB1-containing antibodies from donor A.

Shown are the sequences of antibodies isolated from MDA (donor A). Cryptic splicing sites (GT-AG) are marked in bold blue; alternative splicing sites are marked in bold red. MDA8 employs a different splicing site in the intron between LILRB1 exon 7 encoding the D3 domain and the exon 8 encoding the D4 domain, resulting in insertion of a piece of intronic sequence (originated from the intron between exon 7 and 8) before the exon 8.

a

V(D)J   D3   D4

b

V(D)J   D3   D4

c

d

V(D)J   D3

e

Extended Data Fig. 2. Alignment of cDNA and amino acid sequences of LILRB1-containing antibodies from three donors.

a, Protein sequences from MDA (donor A). **b**, cDNA sequence from MDB (donor B). **c**, Protein sequence from MDB. **d**, cDNA sequences from MDC (donor C). **e**, Protein sequences from MDC. Mutation in the D3 domain (p.Y291D) is highlighted in red.

a

MDA1: Sμ-intron-exon6-intron-exon7(D3)-intron-exon8(D4)-intron-Sμ-Sγ1

```
CTCAAGATGTTTTAATGACTTTAAAGCAGCAAAGAAATATTCCACCCAGGTAGTGGAGGGTGGTAATGATTGGTAATGCTTTGGAA
CCAAAACCCAGGTGGCGCTGGGGCAGGACTGCAGGGAACTGGGGTATCAAGTAGAGGGAGACAAAAGATGGAAGCCAGCCTGGCTG
TGCAGGAACCCGGCAATGAGATGGCTTTTGCCCGTGGGTCGTCCCGCGCCATCTTCTCCGTGGGCCCCGTGAGCCCGAGTCGCAGG
TGGTGGTACAGGTGCTATGCTTATGACTCGAACTCTCCCTATGAGTGGTCTCTACCCAGTGATCTCCTGGAGTTCCTGGTCCTAGG
TGAGAAATTCACAGCATTGCCTGGAGTTCCCTGAGTCTCCAGGCAGGTGGGGAGCAGCCGCGTCTCAGGGCAGTTCCAGGTGGGAT
GATGTTGGGGCGAGAGGGCTCAGGGCTCCTGGGGCCAGAGACACAGGAAGATCAGCAGTGATGTGGCCCCGGGGGAAAGGGAAGAT
TTGTGGGGAAGCCTGAGGGTCGGCTCCTGGAAACCATGACCACCTTTTCCCAGGTGTTTCTAAGAAGCCATCACTCTCAGTGCAGC
CAGGTCCTATCGTGGCCCCTGAGGAGACCCTGACTCTGCAGTGTGGCTCTGATGCTGGCTACAACAGATTTGTTCTGTATAAGGAC
GGGGAACGTGACTTCCTTCAGCTCGCTGGCGCACAGCCCCAGGCTGGGCTCTCCCAGGCCAACTTCACCCTGGGCCCTGTGAGCCG
CTCCTACGGGGGCCAGTACAGATGCTACGGTGCACACAACCTCTCCTCCGAGTGGTCGGCCCCCAGCGACCCCCTGGACATCCTGA
TCGCAGGTGAGGAGCCCAGCGGGTTCAGTCAGGGACCCAGGCTCCGCACAGGCCCTGCCGGGGGACCTCAGGTAGTGATGGCCGGG
ATGAGGGATGGGGGTCCCAAGGGAGGGAGAGACAGACAGAGACAGGGGATGGGCGGGGAGGGGGAGACTCAGAGAAAACAGAGACA
GAGACACTGAGGGTCCCAGAGGGAGACGTTGGGGAGGTGTCAGCTCAGGCTCAGAGCAAGGTGGGGCAGCCCCTCGCCCATCCTTCTTCTCTC
CAGGACAGTTCTATGACAGAGTCTCCCTCTCGGTGCAGCCGGGCCCCACGGTGGCCTCAGGAGAGAACGTGACCCTGCTGTGTCAG
TCACAGGGATGGATGCAAACTTTCCTTCTGACCAAGGAGGGGGCAGCTGATGACCCATGGCGTCTAAGATCAACGTACCAATCTCA
AAAATACCAGGCTGAATTCCCCATGGGTCCTGTGACCTCAGCCCATGCGGGGACCTACAGGTGCTACGGCTCACAGAGCTCCAAAC
CCTACCTGCTGACTCACCCCAGTGACCCCCTGGAGCTCGTGGTCTCAGGTGGGGGCCTTGACCCTGTCCTCTCTGAGCTCAAAGTC
TGGGCTGAGCGGGTCTGAGCGGGGCTGAGCTGAGCTAGGAGGAGTAGGGGTCAGGCACTGGAGCTCAGGGGACCAGGGCAGAGCAG
CCGCAGGTGAGCAGGGGCAGGTGGGGGGCAGGAGGAGCAGGGGGCAGGCACTGGAGCTCAGGGGACCAGGGCAGAGCAGCCCCAGG
TGAGCAGGGGCAGGTGGGGGGCAGGAGGASCAGGGGG
```

b

MDB1: Sγ1-inverted exon2intron-intron-exon7(D3)-intron-exon8(D4)-intron-exon9-intron-Sγ1

```
CAGCTCCTGGACTTCAGGGGACCAGGGAGGGCATCTGAAGGTGAACAGGGGCCAGTGGGGGGCAGGATGAGCAGGGGGAAGCTCCT
GGAGCTCAGGGAGCCAAGGCAGAGCAGCCGCAGGTCAGCAGGGGCAGGTGGGAAGCATGGGGAGCAGGTGGGCAGCCCCTGGAAGC
AGAGACGCATCTCGCATCCGGCTGTGCCGCCCAGGCTGAGCTGCGTGTGGCAGTGAGCACAGAAGAGAAATGCAGGTGAGAAATTC
ACAGCATTGCCTGGAGTTCCCTGAGTCCCCAGGCAGGTGGGGAGCAGCCGCGTCTCAGAGCAGTCCCAGGTGGGATGATGTTGGGG
CGAGAGGGCTCAGGGCTCCTGGGGCCAGAGACACAGGAAGATCAGCAGTGATGTGGCCCCGGGGGAAAGGGAAGATTTGTGGGGAA
GCCTGAGGGCCGGCTCCTGGAAACCATGACCACCTTTTCCCAGGTGTTTCTAAGAAGCCATCACTCTCAGTGCAGCCAGGTCCTAT
CGTGGCCCCTGAGGAGACCCTGACTCTGCAGTGTGGCTCTGATGCTGGCTACAACAGATTTGTTCTGTATAAGGACGGGGAACGTG
ACTTCCTTCAGCTCGCTGGCGCACAGCCCCAGGCTGGGCTCTCCCAGGCCAACTTCACCCTGGGCCCTGTGAGCCGCTCCTACGGG
GGCCAGTACAGATGCTACGGTGCACACAACCTCTCCTCCGAGTGGTCGGCCCCCAGCGACCCCCTGGACATCCTGATCGCAGGTGA
AGGAGCCCAGCGGGTTCAGTCAGGGACCCAGGCTCCGCACAGGCCCTGCCGGGGGAGCTCAGGTAGTGATGGCCGGGATGAGGGAT
GGGGGTCCCAAGGGAGGGAGAGACAGACAGAGACAGGGGATGGGCGGGGAGGGGGAGACTCAGAGAAAACAGAGACAGAGACACTG
AGGGTCCCAGAGGGAGACCTGGGGAGGTGTCAGCTCAGAGCAAGGTGGGGCAGCCCCTCGCCCATCCTTCTTCTCTCCAGGACAGT
TCTATGACAGAGTCTCCCTCTCGGTGCAGCCGGGCCCCACGGTGGCCTCAGGAGGAACGTGACCCTGCTGTGTCAGTCACAGGGA
TGGATGCAAACTTTCCTTCTGACCAAGGAGGGGGCAGCTGATGACCCATGGCGTCTAAGATCAACGTACCAATCTCAAAAATACCA
GGCTGAATTCCCCATGGGTCCTGTGACCTCAGCCCATGCGGGGACCTACAGGTGCTACGGCTCACAGAGCTCCAAACCCTACCTGC
TGACTCACCCCAGTGACCCCCTGGAGCTCGTGGTCTCAGGTGGGGGCCTTGACCCTGTCCTCTCTGAGCTCAAAGTCTCAGCTCAG
ACCCTGCCCCAGGAGAGCTCTGGGCTGGGATGGGAGTGAGCGGGGGTCTGAGAGGGGGCTCAGCCAGTGGGAGACTCACCCTCAGAGG
GAAGGAGGAGAACAGGGCCCTCCCAGGCCTGCCCACCCTCAGTGGCATCGCCAGCATCATGGACAGGAGGAGGCGGGTGGAGGGAGG
GGCCTGGGGAGGCCACAGGTCCCATGTAGAGAAATTTGGTTTGAGGTGGAGACTTCAGGAAAGCCCCAGCTCCTCAGCCTCCTCTC
ATTCTTTTACCCAGGACCGTCTGGGGGCCCCAGCTCCCCGACAACAGGCCCCACCTCCACATCTGGTGAGTCCCTCGAGGCTTCTGA
ACTCAAGGGAGTGCGGCCTCCCCCAGGGCAGCCCTGGGTCTCCCAGAGAATCCCATTCCCCTCAAAGACTCGAGCTTCCCTCCAGG
GAGCCGGGCAGAGCCAGAGGAGGGGCCACAGGGTCCCCAGGGCTCTGAGGCTGGGCTGGTGAGGGGTGGGGGGTCAAGGCAGAGAG
GAGAGCCAGGGCAGATCATCCACAGGAGAGCAGGGGCTGGTAGGAAGCAGGAGGAGCAAGTGGGCAGCTTTTGGAGCTCAGAGCAC
CAGGGCAGAAGAGCCTCAGGTGAGAAGGGGCAGGTG
```

c

MDC1: Sμ-exon6-intron-exon7(D3)-intron-Sμ

Protein: Y to D mutation at 291aa

```
TGGGCTGGGCTGAGCTGGGCTGGGCTGGGCTGGGCTGAACGGGTCTGAGCGGGGCTGAGCTGAGCTAGGCTGGGCTGGGCTGAGCT
GGGCTGAGCTGGGCTGAGCTGGGCTGAGCAAGGCTAGGCTGAGCTGGGCTGAGCTGAGCTGGGCCGAGCTCAGCAGAGCTGAGCCG
AGCTGAGCTTAGCTGGGCTGAGCTAACCAGCCCGAGTCGCAGGTGGTGGTACAGGTGCTATRCTTATGACTCGAACTCTCCCTATG
AGTGGTCTCTACCCAGTGATCTCCTGGAGCTCCTGGTCCTAGGTGAGAAATTCACAGCATTGCCTGGAGTTCCCTGAGTCTCCAGG
CAGGTGGGGAGCAGCCGCGTCTCAGGGCAGTTCCAGGTGGGATGATGTTGGGGCGAGAGGGCTCAGGGCTCCTGGGGCCAGAGACA
CAGGAAGATCAGCAGTGATGTGGCCCCGGGGGAAAGGGAAGATTTGTGGGGAAGCCTGAGGGTCGGCYCCTGGAAACCATGACCAC
CTTTTCCCAGGTGTTTCTAAGAAGCCATCACTCTCAGTGCAGCCAGGTCCTATCGTGGCCCCTGAGGAGACCCTGACTCTGCAGTG
TGGCTCTGATGCTGGCTACAACAGATTTGTTCTGTATAAGGACGGGGAACGTGACTTCCTTCAGCTCGCTGGCGCACAGCCCCAGG
CTGGGCTCTCCCAGGCCAACTTCACCCTGGGCCCTGTGAGCCGCTCCGACGGGGGCCAGTACAGATGCTACGGTGCACACAACCTC
TCCTCCGAGTGGTCGGCCCCCAGTGACCCCCTGGACATCCTGATCGCAGGTGAGGAGCCCAGCGGGTTCAGATGAGCTGAACTGGG
CAGAACGGACTGAGGCGAGCAGGGCCGAGCTGAGCAGAGCTAAGCCGAGGCTGGGCTGGGCTAACCTGGGCTGGGCCGAGTTGAGC
AGAGCTAAGCCGAGGCTGGGCTGGGCTTACCTGGGCTGGGCTGAGCTGAGCTGGGTTGGGCAGGGCTGGGCTGGGCTGAGCTAAGC
TGAACTAGGGTGA
```

Reference genome (Chr 14, GRCCh38. assembly)

LILRB1_205(Ensembl,20.371kb)

Inverted intron-exon-2: 13325..13402

Extended Data Fig. 3. Analysis of genomic sequences of the junction of switch regions containing LILRB1 domains from one representative clone of each donor.
a, MDA (donor A). **b**, MDB (donor B), the gene coordinates of the inserted exon 2 are indicated in red at the bottom. **c**, MDC (donor C). The annotations are color coded as shown in the beginning of each penal. The reference sequences used are indicated at the bottom.
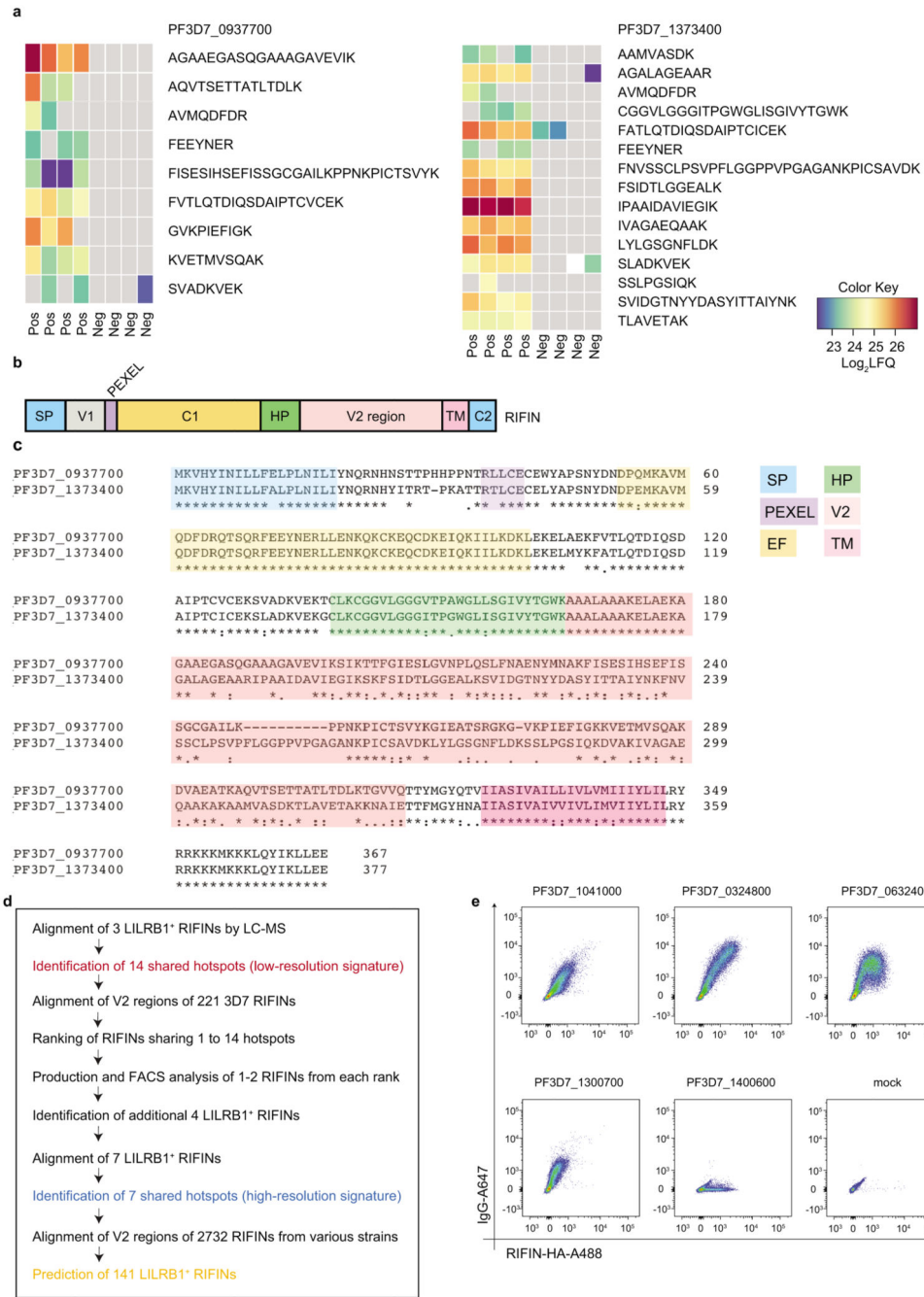
Extended Data Fig. 4. Identification of specific RIFINs recognized by MDB1 antibody.
a, Heatmap showing the enrichment of peptides in 3D7-MDB1+ IEs from the LC-MS/MS analysis, color key indicates the value of Log_2LFQ (relative label-free quantification) intensity, the higher the value, the stronger the signal. **b**, Representation of RIFIN protein. RIFIN has two major conserved constant regions 1 and 2 (C1, C2), as well as two major variable regions (V1, V2). SP, signal peptide; V, variable region; PEXEL, PEXEL motif; HP, hydrophobic Patch; C, constant region; TM, transmembrane region. The images are not drawn to scale. **c**, Alignment of representative full length RIFINs protein (PF3D7_0937700,

PF3D7_1373400) and the definition of the V2 domain (coral pink). EF-hang motif (EF) is a part of C1 region defined by sequence alignment (highlight in color yellow). The legends are the same as in panel **b**. **d**, Workflow to identify additional RIFINs recognized by LILRB1-containing antibodies. Prediction of 141 LILRB1^{+} RIFINs from various strains can be found in Source Data Extended Fig. 4 marked in yellow. **e**, FACS analysis of four additional LILRB1-binding RIFINs expressed on HEK293F transfectants stained with MDB1 antibody. LAIR-binding RIFIN PF3D7_1400600 is included as a control.
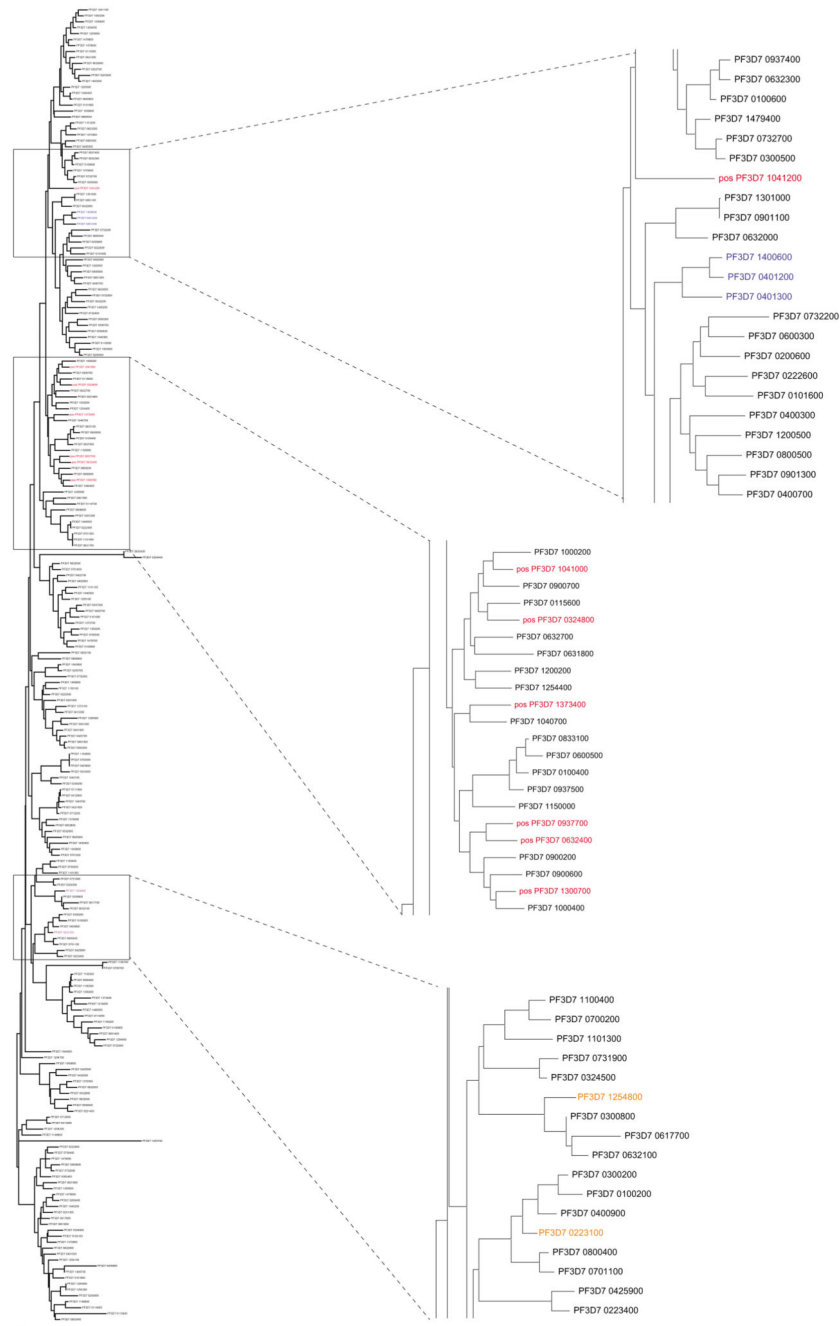
Extended Data Fig. 5. 3D7 RIFIN V2 phylogenetic tree.

Phylogenetic tree of 221 3D7 RIFIN V2 sequences. LILRB1^{+} RIFINs are highlighted in red. LAIR1^{+} RIFINs are highlighted in blue. Previously reported two LILRB1^{+} RIFINs are highlighted in orange.
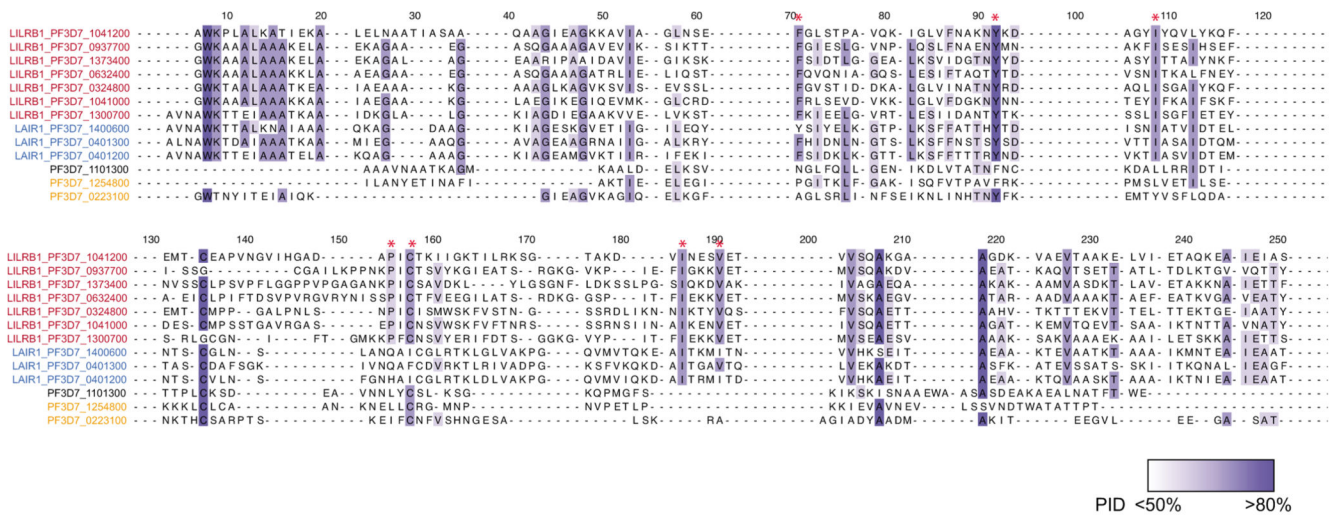

Extended Data Fig. 6. 3D7 RIFIN V2 homology analysis.

Homology analysis of LILRB1^{+} RIFINs and other RIFINs (RIFINs are colored coded as in Extended Data Fig. 5). Seven shared signatures among LILRB1^{+} RIFINs are marked with red asterisk. Amino acid conservation is shown in gradient blue (darker indicates higher conservation). PID, percentage identity.
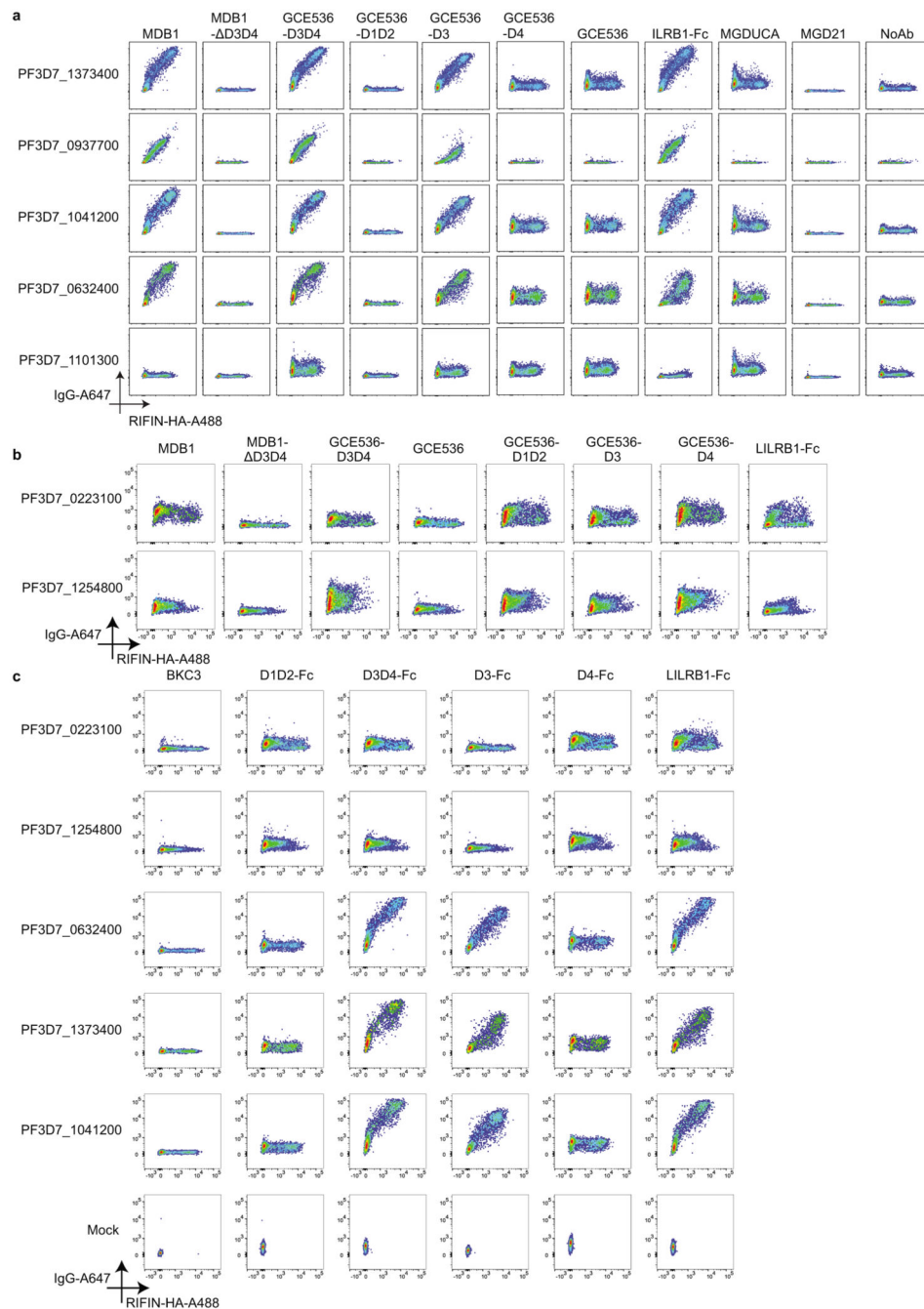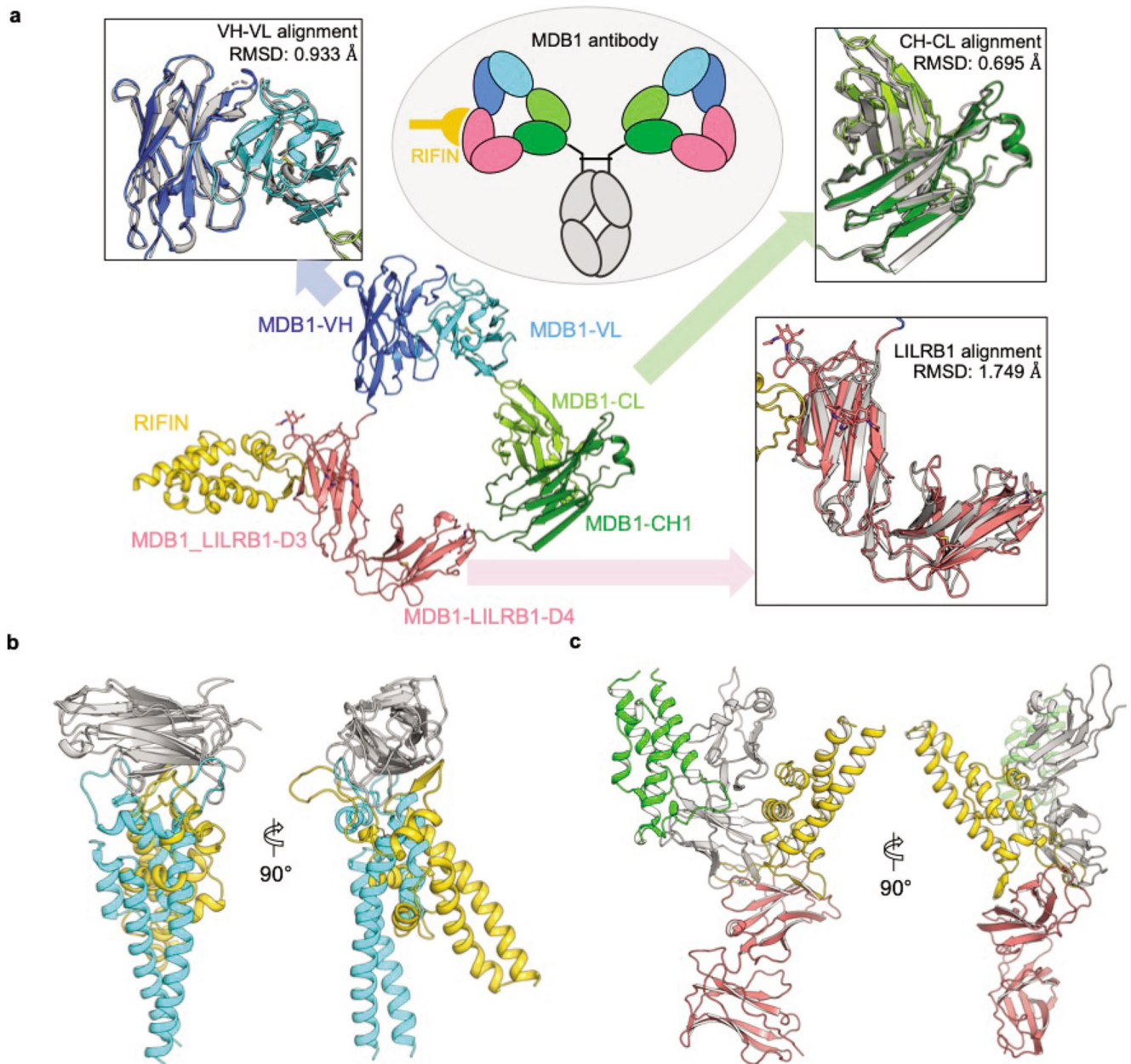
Extended Data Fig. 7. Representative FACS plots of RIFINs binding to various constructs.
a-b, FACS analysis of representative RIFINs binding to natural or recombinant antibodies or control antibodies (representative of $n = 3$ independent experiments). **c**, FACS analysis of representative RIFINs binding to Fc fusion proteins containing LILRB1 domain/domains (representative of $n = 2$ independent experiments).
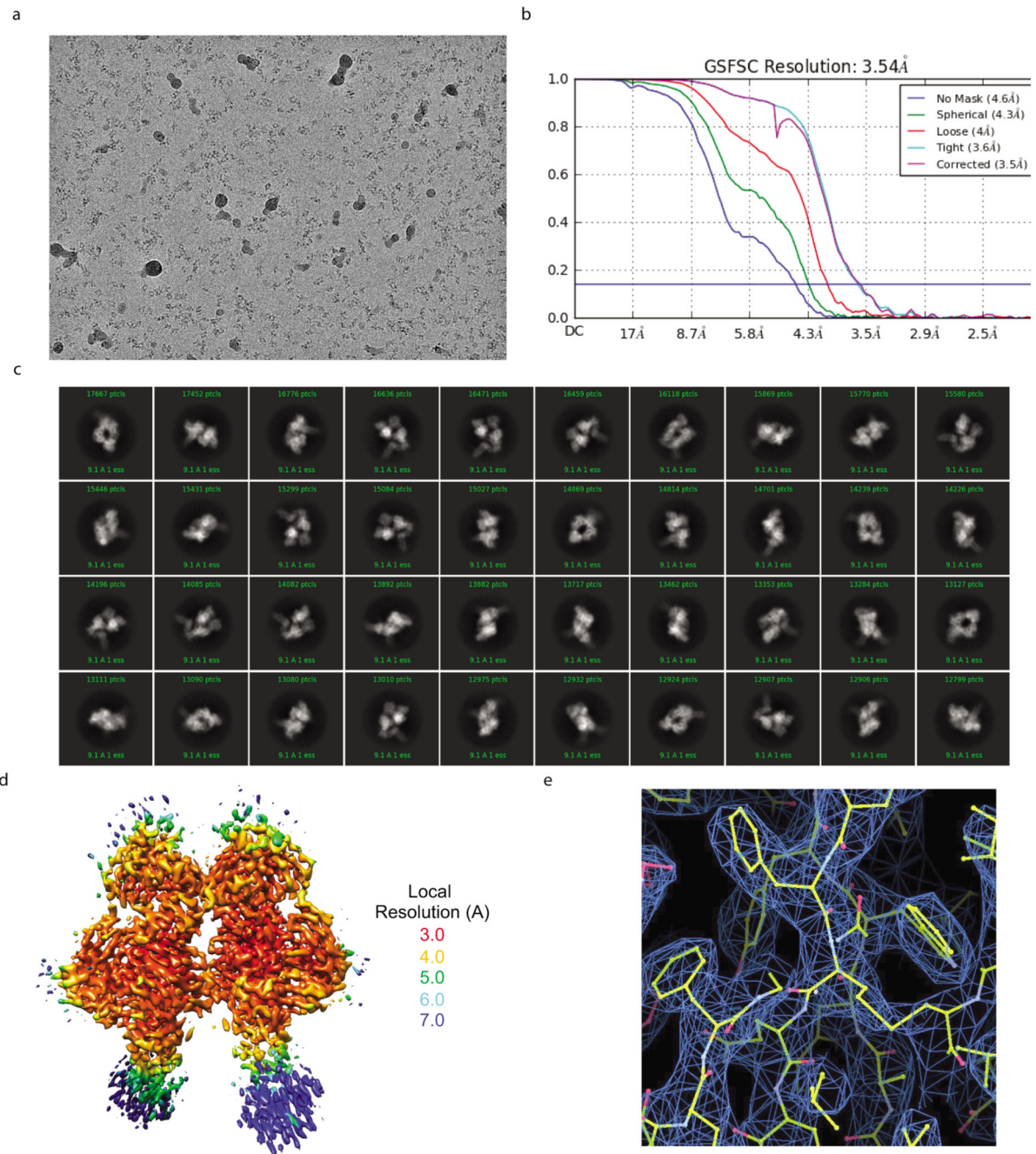
Extended Data Fig. 8. Cryo-EM data processing and validation.
a, A representative cryo-EM micrograph showing MDB1-RIFIN complex embedded in vitreous ice. **b**, Overall resolution estimation (FSC, 0.143). **c**, Representative 2D average classes. **d**, Local resolution estimation of the cryo-EM map. **e**, Cryo-EM density and refined models for a representative region.

Extended Data Fig. 9. Structural analysis MDB1 and various modes of RIFIN-receptor interaction.
a, Triangular architecture of LILRB1-containing MDB1 antibody Fab and structural comparison. Inside the ellipse it shown a schematic view of MDB1 with RIFIN attached to one arm of the Fab. The insets show structural superimposition of MDB1 domains to a non-inserted antibody and to apo LILRB1 (upper left: VH-VL region aligned with PDB 6P3B; upper right: CH-CL region aligned with PDB 6P3B; bottom right: LILRB1 insertion aligned with PDB 4LLA). **b**, Comparison of LILRB1/LAIR1 (grey) recognition by RIFIN PF3D7_1373400 (yellow) and RIFIN PF3D7_1040300 (PDB 7JZI, cyan), respectively. **c**,

Comparison of LILRB1 (D1D2 in grey, D3D4 in red) recognition by RIFIN PF3D7_1254800 (PDB 6ZDX, green) and RIFIN PF3D7_1373400 (yellow).
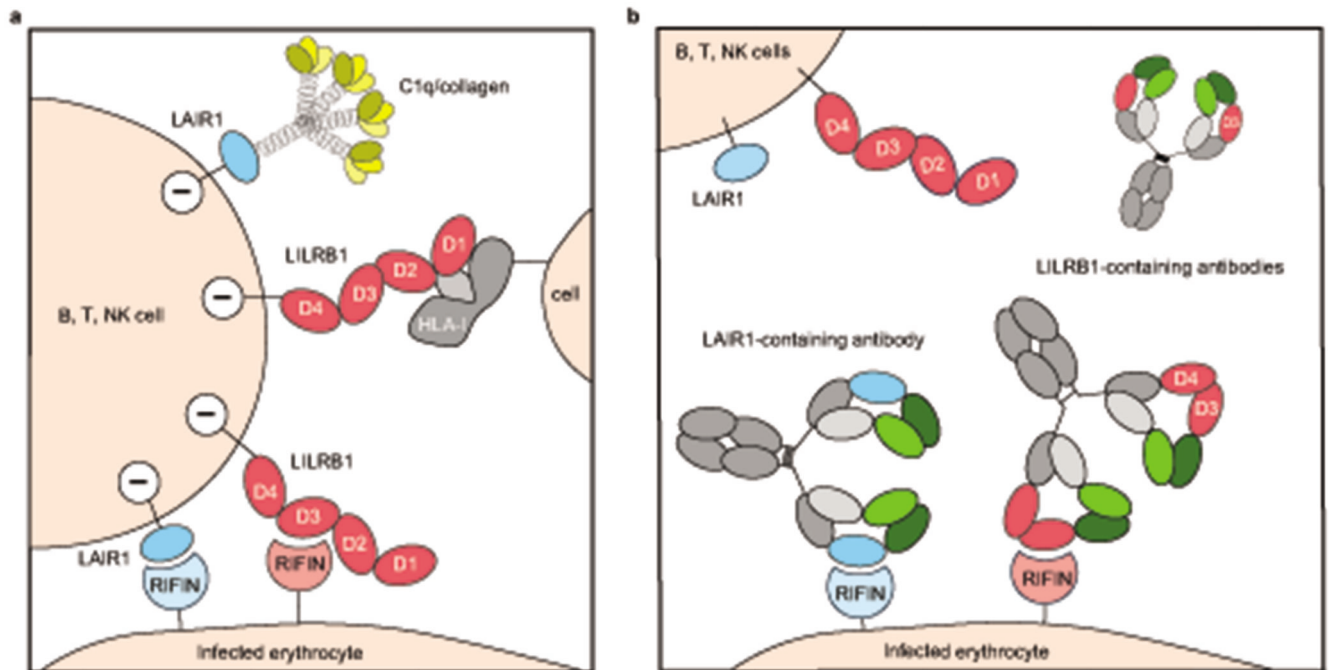
Extended Data Fig. 10. Scheme of receptor-based antibodies hijacking binding of RIFIN to host inhibitory receptors.

a, Immune cells such as B, T, Natural Killer cells express inhibitory receptors LILRB1 or LAIR1 on the cell surface. Infected erythrocytes (IEs) express surface variant antigen RIFINs that can target host inhibitory receptors such as LILRB1 or LAIR1 for immune invasion. Cross-linking of HLA-1 on cells with the LILRB1 D1D2 domain can deliver a negative regulatory signal to the LILRB1 expressing cells. LAIR1 binds to C1q or collagen like domains. LAIR1, bule; C1q, yellow; LILRB1, red; HLA-I, gray; LILRB1 specific RIFIN, light pink; LAIR1 specific RIFIN, light blue. **b**, Host immune system developed natural receptor-based antibodies to combat this evasion mechanism employed by IEs. LILRB1-containing antibody does not cross-react with RIFINs that are specific for LAIR1. Antibody heavy chain VH, dark green; constant region CH, gray; light chain VL, light green; light chain constant CL, light gray.

Supplementary Material

Refer to Web version on PubMed Central for supplementary material.

Acknowledgements

Data availability

Sequence data for the monoclonal antibodies isolated in this study have been deposited in GeneBank (NCBI) with the accession codes MT897911 for MDA1, MT897912 for MDB1 and MT897913 for MDC1. The mass spectrometry differential expression data and MaxQuant search results can be found in Source Data Fig. 2. A list of tested RIFINs is also presented in Source Data Fig. 2. LILRB1 binding RIFIN prediction data from various parasite strains is presented in the Source Data Extended Data Fig. 4. The crystal structure of LILRB1 D3D4 domain in complex with RIFIN PF3D7_1373400 V2 domain has been deposited in the Protein Data Bank (PDB) with accession number 7KFK. All other data are available from the corresponding author on request or in the **Source Data** section.

References

1. Goel S, et al. RIFINs are adhesins implicated in severe Plasmodium falciparum malaria. Nat Med. 2015; 21:314–321. [PubMed: 25751816]

2. Tan J, et al. A LAIR1 insertion generates broadly reactive antibodies against malaria variant antigens. Nature. 2016; 529:105–109. [PubMed: 26700814]

3. Pieper K, et al. Public antibodies to malaria antigens generated by two LAIR1 insertion modalities. Nature. 2017; 548:597–601. [PubMed: 28847005]

4. Chapman TL, Heikema AP, West AP, Bjorkman PJ. Crystal structure and ligand binding properties of the D1D2 region of the inhibitory receptor LIR-1 (ILT2). Immunity. 2000; 13:727–736. [PubMed: 11114384]

5. Harrison TE, et al. Structural basis for RIFIN-mediated activation of LILRB1 in malaria. Nature. 2020; 587:309–312. [PubMed: 32650338]

6. Wahlgren M, Goel S, Akhouri RR. Variant surface antigens of Plasmodium falciparum and their roles in severe malaria. Nat Rev Microbiol. 2017; 15:479–491. [PubMed: 28603279]

7. Saito F, et al. Immune evasion of Plasmodium falciparum by RIFIN via inhibitory receptors. Nature. 2017; 9:1–22.

8. Arama C, et al. Ethnic differences in susceptibility to malaria: What have we learned from immuno-epidemiological studies in West Africa? Acta Trop. 2015; 146:152–156. [PubMed: 25820030]

9. Koning MT, et al. Templated Insertions at VD and DJ junctions Create Unique B-Cell Receptors in the Healthy B-Cell Repertoire. Eur J Immunol. 2020; 50:2099–2101. [PubMed: 32762049]

10. Higgins MK, Carrington M. Sequence variation and structural conservation allows development of novel function and immune evasion in parasite surface protein families. Protein Sci. 2014; 23:354–365. [PubMed: 24442723]

11. Tran TM, et al. An intensive longitudinal cohort study of malian children and adults reveals no evidence of acquired immunity to plasmodium falciparum infection. Clin Infect Dis. 2013; 57:40–47. [PubMed: 23487390]

12. Tiller T, et al. Efficient generation of monoclonal antibodies from single human B cells by single cell RT-PCR and expression vector cloning. J Immunol Methods. 2008; 329:112–124. [PubMed: 17996249]

13. Rieckmann JC, et al. Social network architecture of human immune cells unveiled by quantitative proteomics. Nat Immunol. 2017; 18:583–593. [PubMed: 28263321]

14. Cox J, Mann M. MaxQuant enables high peptide identification rates, individualized p.p.b.-range mass accuracies and proteome-wide protein quantification. Nat Biotechnol. 2008; 26:1367–1372. [PubMed: 19029910]

15. Wheeler DL, et al. Database resources of the National Center for Biotechnology Information. Nucleic Acids Res. 2007; 35:5–12.

16. Sievers F, Higgins DG. Clustal Omega. Curr Protoc Bioinforma. 2014; 2014

17. Kumar S, Stecher G, Li M, Knyaz C, Tamura K. MEGA X: Molecular evolutionary genetics analysis across computing platforms. Mol Biol Evol. 2018; 35:1547–1549. [PubMed: 29722887]

18. Suloway C, et al. Automated molecular microscopy: The new Leginon system. J Struct Biol. 2005; 151:41–60. [PubMed: 15890530]

19. Punjani A, Rubinstein JL, Fleet DJ, Brubaker MA. CryoSPARC: Algorithms for rapid unsupervised cryo-EM structure determination. Nat Methods. 2017; 14:290–296. [PubMed: 28165473]

20. Pettersen EF, et al. UCSF Chimera - A visualization system for exploratory research and analysis. J Comput Chem. 2004; 25:1605–1612. [PubMed: 15264254]

21. Emsley P, Cowtan K. Coot: Model-building tools for molecular graphics. Acta Crystallogr Sect D Biol Crystallogr. 2004; 60:2126–2132. [PubMed: 15572765]

22. Adams PD, et al. PHENIX: A comprehensive Python-based system for macromolecular structure solution. Acta Crystallogr Sect D Biol Crystallogr. 2010; 66:213–221. [PubMed: 20124702]

23. Davis IW, et al. MolProbity: All-atom contacts and structure validation for proteins and nucleic acids. Nucleic Acids Res. 2007; 35:375–383.

24. Barad BA, et al. EMRinger: Side chain-directed model and map validation for 3D cryo-electron microscopy. Nat Methods. 2015; 12:943–946. [PubMed: 26280328]
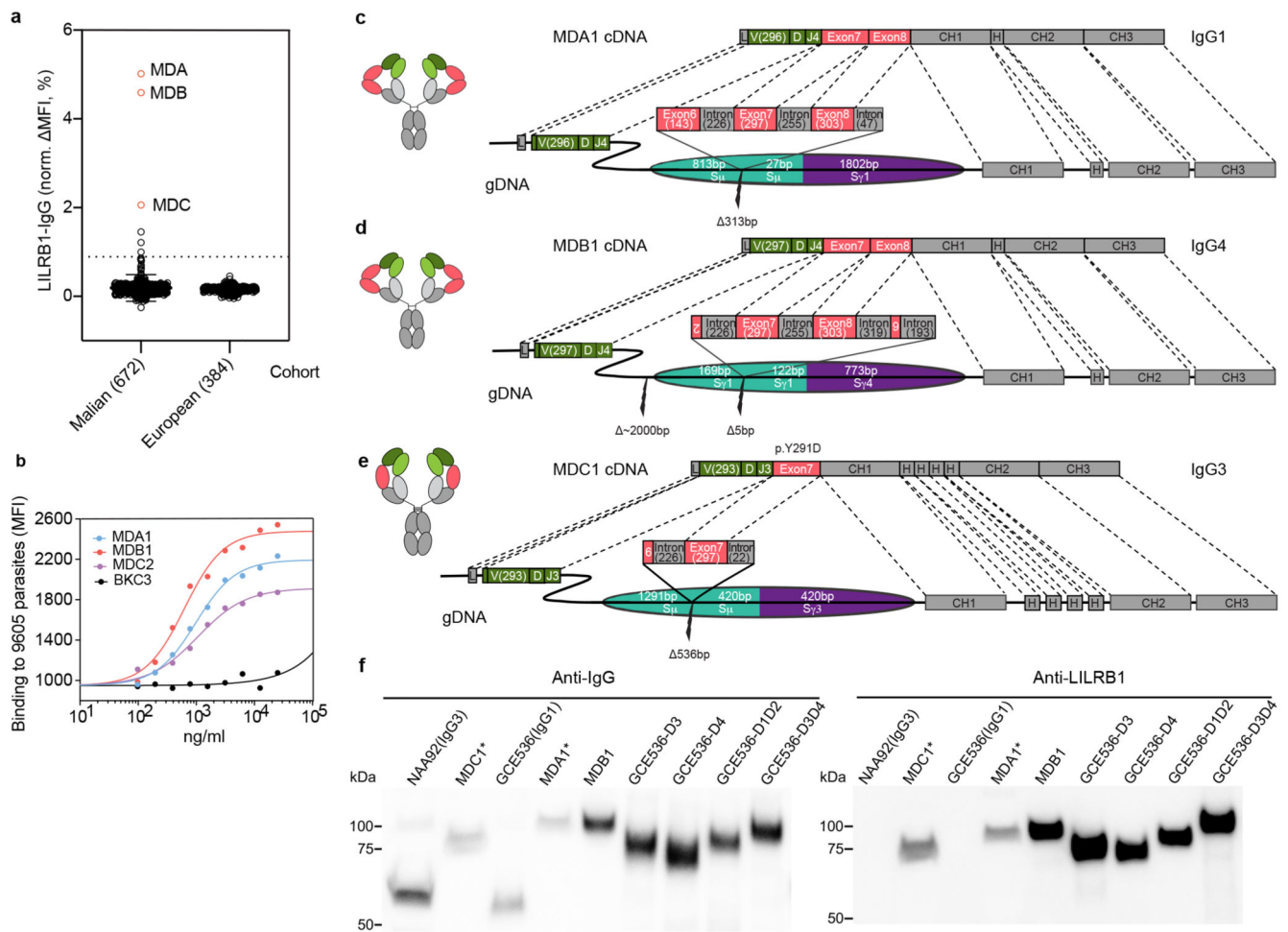
Fig. 1. Isolation and identification of LILRB1-containing antibodies from a Malian cohort.
a, Prevalence of LILRB1-containing IgG in plasma of Malian donors compared to a control cohort of European individuals. Donors from whom LILRB1-containing antibodies were isolated are shown in red. The error bars indicate the standard deviation. A cutoff set at normalized ΔMFI = 1% was used to identify donors with detectable levels of LILRB1-containing antibodies. **b**, Binding of LILRB1-containing monoclonal antibodies to erythrocyte infected by the 9605 parasite isolate (representative of $n = 3$ independent experiments). An antibody of irrelevant specificity was used as negative control (BKC3). **c-e**, cDNA and genomic DNA organization in representative B cell clones from 3 donors. LILRB1 inserted DNA segments are colored in red (exons) or dark gray (introns); numbers in brackets indicate the length of inserted nucleotides; adjacent switch regions are shown in teal and purple. Antibody variable domain (VH), green; light chain (VL), light green; CH, dark gray; CL, light gray. **f**, Western blot analysis of naturally occurring LILRB1-containing antibodies (MDC1 and MDA1 tested as culture supernatants and MDB1 tested as recombinant antibody). Shown are also IgG1 and IgG3 isotype control antibodies (GCE536 and NAA92), as well as recombinant antibodies carrying different LILRB1 domains inserted in the GCE536 VH-CH1 elbow (representative of $n = 2$ independent experiments). For gel source data, see Supplementary Fig. 1.
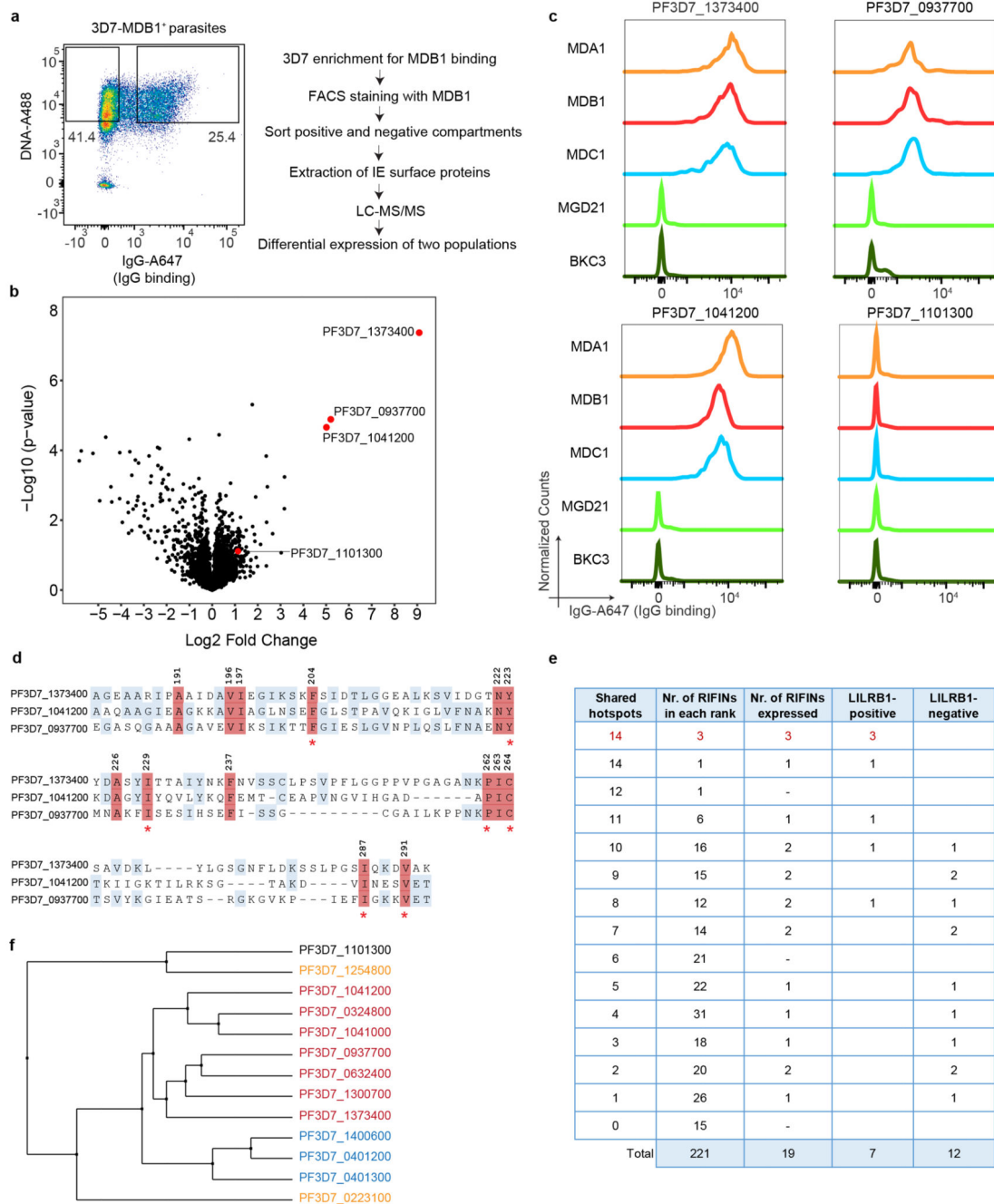
Panel e table:

Shared hotspots	Nr. of RIFINs in each rank	Nr. of RIFINs expressed	LILRB1-positive	LILRB1-negative
14	3	3	3	
14	1	1	1	
12	1	-		
11	6	1	1	
10	16	2	1	1
9	15	2		2
8	12	2	1	1
7	14	2		2
6	21	-		
5	22	1		1
4	31	1		1
3	18	1		1
2	20	2		2
1	26	1		1
0	15	-		
Total	221	19	7	12

Fig. 2. LILRB1-containing antibodies bind to distinct RIFINs.

a, Workflow of the sorting strategy and proteomics pipeline to identify proteins differentially expressed in MDB1^{+} and MDB1^{-} 3D7 IEs. **b**, Volcano plot showing differentially expressed 3D7 *P. falciparum* proteins in MDB1^{+} versus MDB1^{-} IEs, as determined by the LC-MS/MS analysis (from $n = 4$ independent experiments). Statistical significance was evaluated by Welch tests. **c**, Staining of HEK293F cells transfected with high-score RIFINs (PF3D7_1373400, PF3D7_0937700 and PF3D7_1041200), or a low-score RIFIN (PF3D7_1101300) using LILRB1-containing antibodies (MDA1, MDB1, MDC1), a LAIR1-

containing antibody (MGD21) or an irrelevant control antibody (BKC3) (representative of *n* = 3 independent experiments). **d**, Alignment of the 3 positive RIFINs identifies a 14-residue shared signature (highlighted in red). Residue numbering refers to RIFIN PF3D7_1373400. Homologies are highlighted in blue. **e**, 221 3D7 RIFINs were ranked according to the number of hotspots shared with the 14-residue signature of the 3 positive RIFINs identified by proteomics. Shown is the number of RIFINs in each rank, the number of RIFINs successfully expressed as V2-domains on HEK293F cells and their staining by a LILRB1 antibody (MDB1). The 4 new LILRB1-specific RIFINs identified a higher resolution signature based on 7 shared hotspots which are marked with an asterix in **d**. **f**, Phylogenetic tree showing distance between LILRB1+ RIFINs (red), LAIR1+ RIFINs (blue), previously reported LILRB1-binding RIFINs (orange) or a non-LILRB1 binding RIFIN (black). Trees are calculated by the PAM250 score matrix, which indicates a global similarity score between any two sequences.
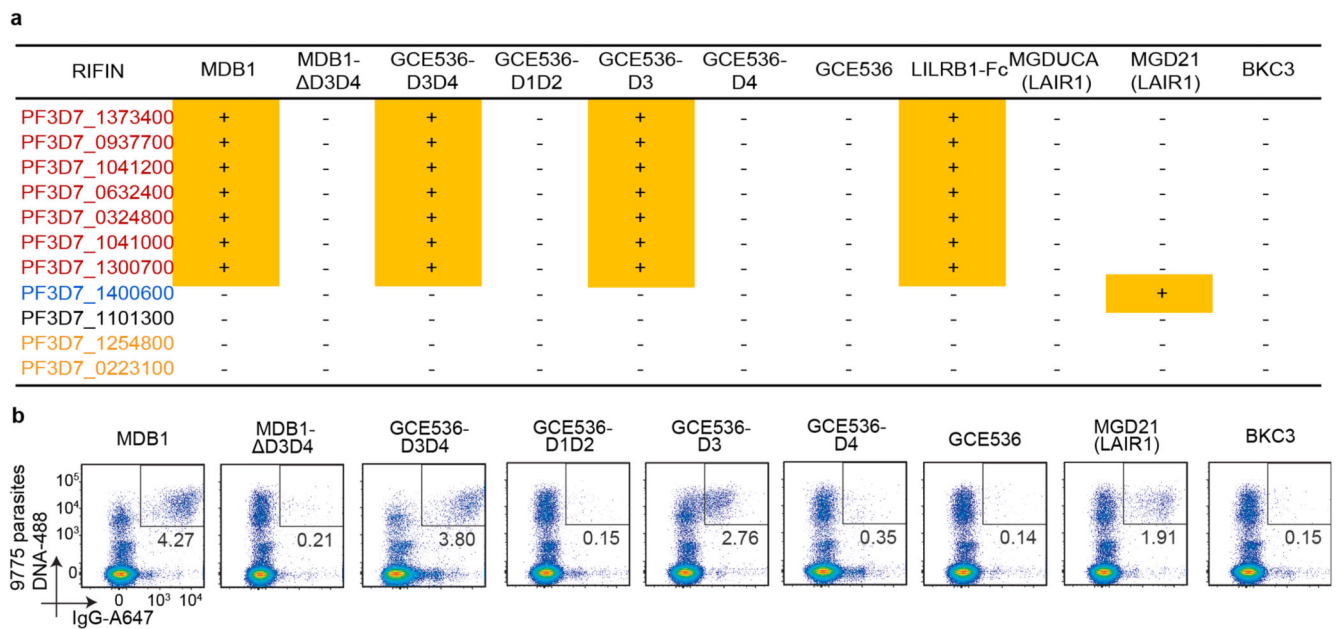
a

RIFIN	MDB1	MDB1-ΔD3D4	GCE536-D3D4	GCE536-D1D2	GCE536-D3	GCE536-D4	GCE536	LILRB1-Fc	MGDUCA (LAIR1)	MGD21 (LAIR1)	BKC3
PF3D7_1373400	+	-	+	-	+	-	-	+	-	-	-
PF3D7_0937700	+	-	+	-	+	-	-	+	-	-	-
PF3D7_1041200	+	-	+	-	+	-	-	+	-	-	-
PF3D7_0632400	+	-	+	-	+	-	-	+	-	-	-
PF3D7_0324800	+	-	+	-	+	-	-	+	-	-	-
PF3D7_1041000	+	-	+	-	+	-	-	+	-	-	-
PF3D7_1300700	+	-	+	-	+	-	-	+	-	-	-
PF3D7_1400600	-	-	-	-	-	-	-	-	-	+	-
PF3D7_1101300	-	-	-	-	-	-	-	-	-	-	-
PF3D7_1254800	-	-	-	-	-	-	-	-	-	-	-
PF3D7_0223100	-	-	-	-	-	-	-	-	-	-	-

b

Fig. 3. The LILRB1 extracellular domain 3 (D3) is responsible for binding to a set of RIFINs. **a**, Identification of LILRB1 minimum binding domain by staining of selected RIFIN transfectants with natural (MDB1) and recombinant LILRB1-containing antibodies (GCE536-D3D4, GCE536-D1D2, GCE536-D3, and GCE536-D4), and controls (MDB1 lacking D3D4 domains, GCE536, the fusion protein LILRB1-Fc and LAIR1-containing antibodies MGD21 or germline reverted MGDUCA). RIFINs are color coded as shown in Fig. 2f. RIFINs which showed positive binding specificities were indicated in yellow rectangle with a "+" inside, otherwise were marked with a "-". (representative of $n = 3$ independent experiments). **b**, Example of staining of parasite isolate 9775 with natural and recombinant LILRB1-containing antibodies, or with control antibodies (representative of $n = 3$ independent experiments).
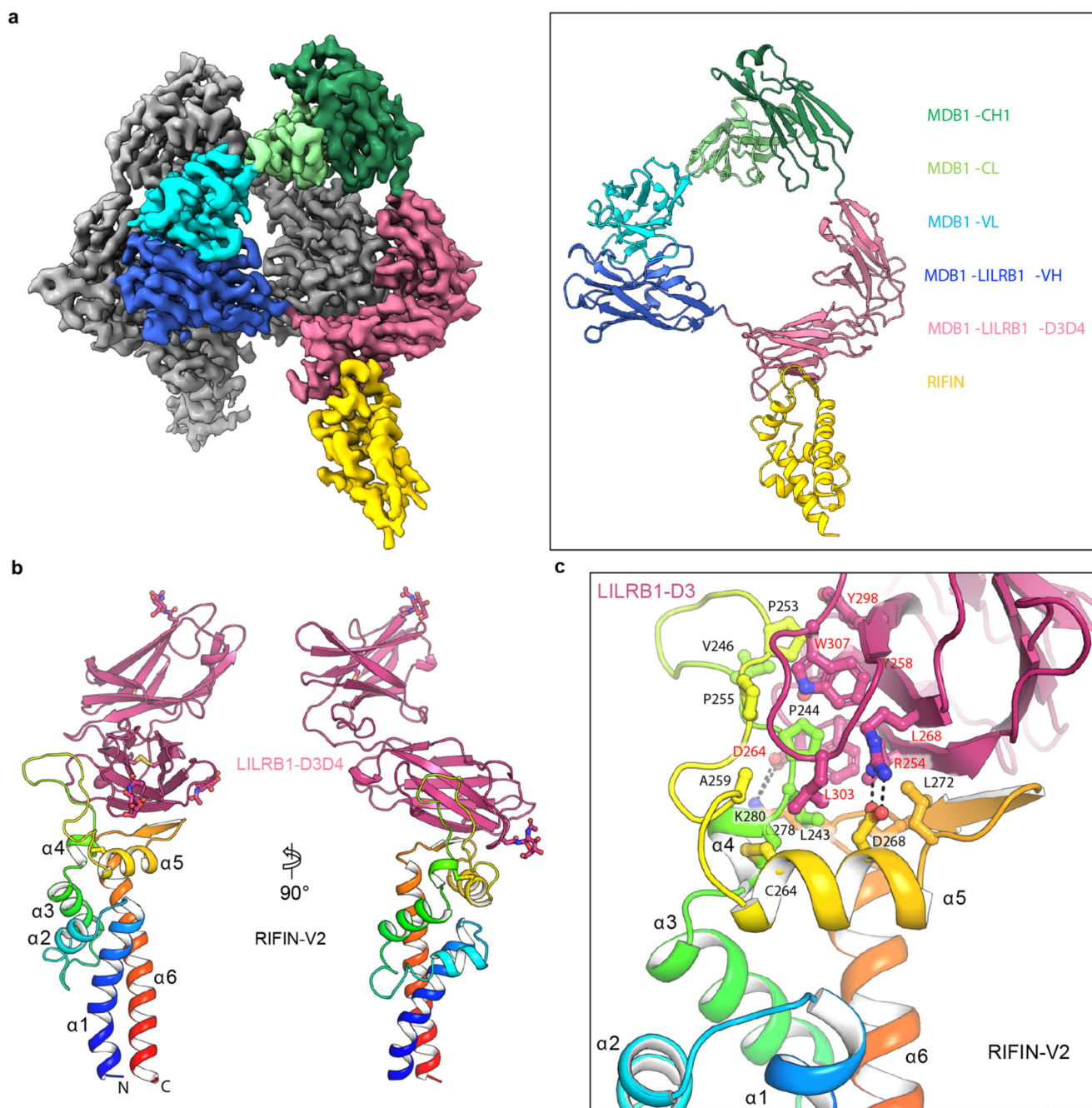
Fig. 4. Structure basis of RIFIN recognition by MDB1 antibody and LILRB1 receptor.
a, Cryo-EM structure of RIFIN-V2 (PF3D7_1373400) domain in complex with MDB1 Fab. Left panel shows sharpened cryo-EM density map of RIFIN-MDB1 complex in a dimeric assembly with one protomer colored. Right panel shows structure of one RIFIN-MDB1 protomer in cartoon view. Domains are colored individually as indicated in the legend. **b**, Crystal structure of RIFIN-V2 (PF3D7_1373400) domain in complex with LILRB1 D3D4 domains in two orthogonal cartoon views. RIFIN is colored in rainbow and LILRB1 is

colored in red. Atomic model is available with PDB ID 7KFK. **c**, Detailed representation of the interface between RIFIN V2 domain and LILRB1 D3 domain.